The processes of reionization simulated with the LICORICE and 21cmFAST codes

Karolina Zawada[1], **Benoît Semelin**[2]
[1]Toruń Centre of Astronomy, Nicolaus Copernicus University
[2]Laboratoire d'Etude du Rayonnement et de la Matire en Astrophysique
Observatoire de Paris

Key words: *reionization: optical depth, correlation function, differential brightness temperature*

Introduction

One of the possible sources of an anisotropy in the power spectrum of 21 cm brightness fluctuations from the epoch of reionization (EoR) is the delay in light traveltime along the line-of-sight (LOS). We examine the anisotropy between the parallel and transverse directions with respect to the LOS. The inhomogeneous distribution of ionized clouds at the redshift of $z > 6$ should provide an enhanced level of inhomogeneity in the Thomson optical depth. Evolution of the optical depth, the correlation function of ionization field and the differential brightness temperature of the 21 cm signal at the EoR are evaluated with the **LICORICE** and **21cmFAST** codes.

Method, results, conclusions

LICORICE is the Monte-Carlo 3D radiative transfer code, coupled to the dynamics via an adaptative Tree-SPH code. The code includes continuum and Ly-α radiative transfer. Dynamics simulations are made in Gadget-2 code. **21cmFAST** is the semi-numerical code specialized for fast, large-scale simulations of the cosmological 21 cm signal. The results of simulations are transformed from the cartesian coordinates into the grid with the SPH. Calculation of the comoving distance between two

subsequent outputs of the simulation determines the parts of the slices which form the light-cone. Depending on the simulation, the cones have a length of 1.1–2.5 Gpc. Both codes assume flat ΛCDM cosmologies with parameters (size box, grid, h, Ω_Λ, Ω_M): LICORICE: ($100h^{-1}$ Mpc, 256^3, 0.73, 0.76, 0.24) and ($200h^{-1}$ Mpc, 512^3, 0.704, 0.73, 0.27); 21cmFAST: (100Mpc, 100^3, 0.7, 0.72, 0.28) and (400Mpc, 400^3, 0.7, 0.72, 0.28).

Ionization history

The fig.1 shows the unnormalized three dimensional correlation functions of the ionization field at the advanced stages of reionization. The average ionization fraction x_i increases from 18% to 99%. Curves become flat since HII regions start to overlap and the ionization state of IGM becomes more homogeneous.

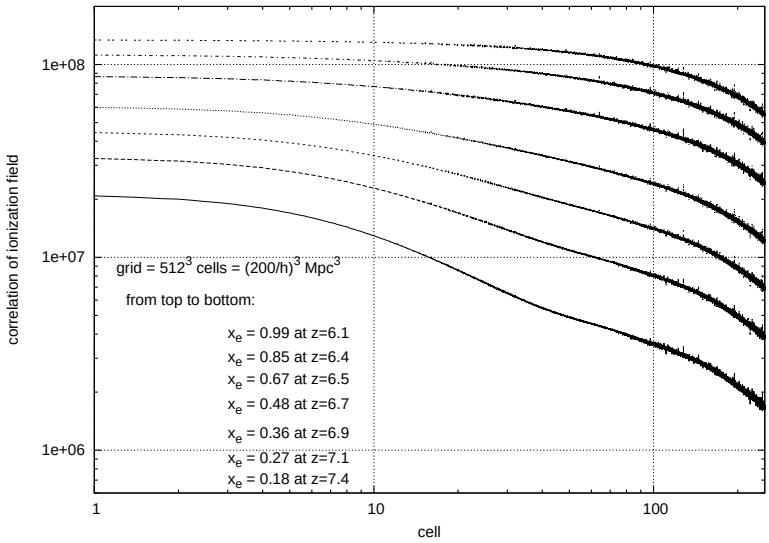

Fig. 1. 3D autocorrelation functions of ionization field for 5 different redshifts with the average ionization fraction x_i. 1 cell is equal to 0.55 Mpc. LICORICE simulation for $200h^{-1}$ Mpc

Source: own work.

Optical depth of the Thomson scattering of CMB photons by free electrons

Reionization history is constrained by the value of τ – the optical depth along the line-of-sight

$$\tau(z) = \frac{c\sigma_T}{H_0}\int_{z_1}^{z_2}\frac{\rho(z)x_i(z)(1+z)^2}{\sqrt{\Omega_M(1+z)^3+\Omega_\Lambda}}dz \qquad (1)$$

where $\rho(z)$ is the density field and $x_i(z)$ is the ionization field. Fig. 2 shows a sample of 2D maps of the total optical depth integrated along the LOS. Integration starts at the moment when first structures came to existence and is calculated to the end of EoR ($z \sim 6$).

All simulation show that the fluctuations of the optical depth τ are substantial, larger than $\pm$ 0.01. This is comparable to the Thomson optical depth along the LOS through the centres of large galaxy clusters. All of the histograms of the 2D simulations calculated for the $100h^{-1}$ Mpc simulations have surprisingly large tails for the higher values of the optical depth compared to histograms for the $200h^{-1}$ Mpc simulations. The most likely explanation is the influence of the box size.

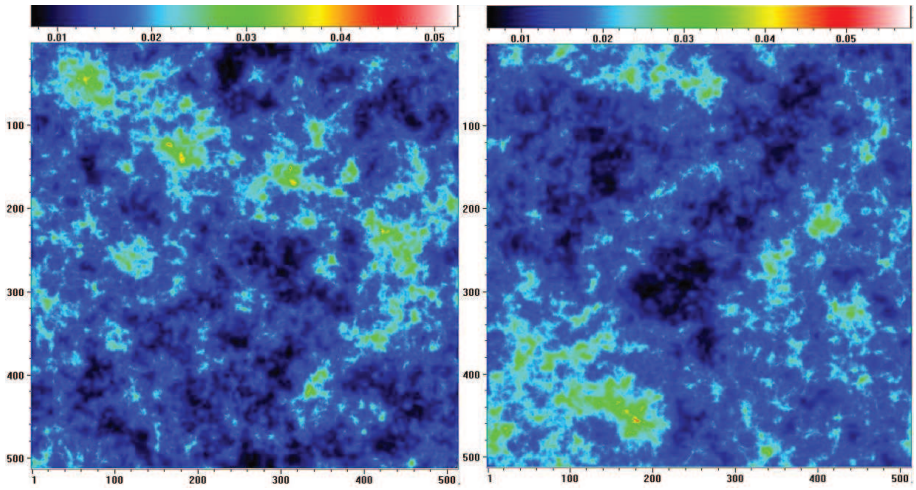

Fig. 2. 2D maps of the total optical depth integrated along the LOS. LICORICE simulation: $200h^{-1}$ Mpc, h=0.704, grid of 512^3 cells. Integration along x (left) and y (right) axis, the longest dimensions of the corresponding light-cones

Source: own work.

Two-point correlation function ξ of 21 cm δT_b

The mean brightness temperature offset δT_b from the CMB temperature at redshift $z = \frac{\nu_0}{\nu} - 1$ is equal to

$$\delta T_b(\nu) = \frac{T_S - T_{CMB}(z)}{1+z}\left(1 - e^{-\tau_{\nu_0}}\right)\ mK \tag{2}$$

where τ_{ν_0} is the optical depth at the 21 cm frequency ν_0 at the diffuse IGM, T_S is spin temperature of the 21 cm gas. The two-point correlation function ξ is a function of the comoving distance r between two points and two redshifts: $\xi = \left\langle \left[\delta T_{b,1} - \delta\bar{T}_b(z_1)\right] \times \left[\delta T_{b,2} - \delta\bar{T}_b(z_2)\right] \right\rangle$. ξ is

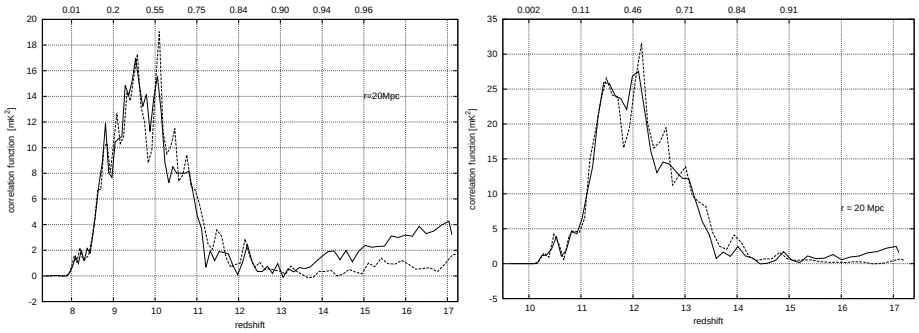

Fig. 3. Two-point correlation function ξ of 21 cm δT_b at the distance of r=20 Mpc as a function of the redshift. The top axis shows the neutral fraction. Solid curves show $\mu = 1$, dashed curves show $\mu = 0$. 21cmFAST simulations are made for 400 Mpc. *Left panel:* Pop2 and *Right panel:* Pop3 stars are sources of reionization

Source: own work.

parametrized as a function of r and $\mu = \cos\Theta$, where $\Theta = 0°$ - along the LOS and $\Theta = 90°$ - perpendicular to the LOS. Redshift z is taken at the mid-point (in terms of comoving distance) of the two points. The mean $\delta\bar{T}_b$ at the appropriate redshifts has been subtracted from δT_b at each point. Results are shown in fig. 3. The correlation is stronger for Pop3 stars model since in that case reionization occurs at a higher redshift and is caused by rarer haloes. Number density of that haloes changes more rapidly with redshift. Early in EoR ξ is low, because ionization affects only the rare high-density regions. Subsequently, density fluctuations enhance fluctuations of ionization fraction what causes increase of ξ. The 21 cm correlation function for comoving distance $r = 20$ Mpc is in agreement with theoretical prediction. We do not observe any strong LOS anisotropy in the ionization fluctuation for bigger values of r (theoretically predicted).

The simulations with $400h^{-1}$ Mpc and full radiative transfer should clearly decouple the influence of the box size from the actual physics effects.

Bibliography

Baek S. *et al.*, 2009, A&A, **495**, 389
Barkana R., Loeb A., 2006, MNRAS, **372**, L43
Doré O. *et al.*, 2007, Phys. Rev. D, **76**, 043002
Mesinger A. *et al.*, 2011, MNRAS, **411**, 955